Bridge-Dependent Electron Transfer in Porphyrin-Based Donor−Bridge−Acceptor Systems

Kristine Kilså,[†] Johan Kajanus,[‡] Alisdair N. Macpherson,[§] Jerker Mårtensson,[‡] and Bo Albinsson*[,†]

Contribution from the Department of Physical Chemistry and Department of Organic Chemistry, Chalmers University of Technology, SE-412 96 Göteborg, Sweden, and Department of Biophysical Chemistry, Umeå University, SE-901 87 Umeå, Sweden

Received October 30, 2000. Revised Manuscript Received February 5, 2001

Abstract: Photoinduced electron transfer in donor−bridge−acceptor systems with zinc porphyrin (or its pyridine complex) as the donor and gold(III) porphyrin as the acceptor has been studied. The porphyrin moieties were covalently linked with geometrically similar bridging chromophores which vary only in electronic structure. Three of the bridges are fully conjugated π-systems and in a fourth, the conjugation is broken. For systems with this bridge, the quenching rate of the singlet excited state of the donor was independent of solvent and corresponded to the rate of singlet energy transfer expected for a Förster mechanism. In contrast, systems with a π-conjugated bridging chromophore show a solvent-dependent quenching rate that suggests electron transfer in the Marcus normal region. This is supported by picosecond transient absorption measurements, which showed formation of the zinc porphyrin radical cation only in systems with π-conjugated bridging chromophores. On the basis of the Marcus and Rehm−Weller equations, an electronic coupling of 5−20 cm^{-1} between the donor and acceptor is estimated for these systems. The largest coupling is found for the systems with the smallest energy gap between the donor and bridge singlet excited states. This is in good agreement with the coupling calculated with quantum mechanical methods, as is the prediction of an almost zero coupling in the systems with a nonconjugated bridging chromophore.

Introduction

Long-range electron transfer (ET) has attracted much attention over the past few decades.[1−4] Areas in which ET plays a major role are, for example, in biological transport systems such as photosynthesis[5,6] and in the construction of artificial photosynthetic complexes,[7−9] solar cells,[10,11] and optoelectronic devices.[12] To understand and gain knowledge of the parameters that control and affect ET, many supramolecular complexes have been synthesized. Recent studies of porphyrin-based systems have focused on geometric parameters (distance and orientation),[13−17] the free energy of reaction,[18−20] and temperature.[21]

The work presented here is part of an ongoing project with the purpose of investigating how the electronic structure of the intervening medium (the bridge in our case) between a donor and an acceptor affects photoinduced energy or electron transfer. To focus solely on this factor, several series of donor−bridge−acceptor (D−B−A) systems, in which the only parameter that is varied within a series is the electronic structure of the bridge, have been investigated. In other words, by keeping the geometric parameters constant, we can determine how the bridging chromophores affect the donor−acceptor electronic coupling. All our series have porphyrin moieties as donor and acceptor, and in previous studies we have focused on singlet−singlet[22,23] and triplet−triplet[24] energy transfer, as well as the enhancement of intersystem crossing in the donor induced by a neighboring

* To whom correspondence should be addressed. E-mail: balb@phc.chalmers.se. Phone: +46-31-772-3044. Fax: +46-31-772-3858.

[†] Department of Physical Chemistry, Chalmers University of Technology.

[‡] Department of Organic Chemistry, Chalmers University of Technology.

[§] Umeå University.

(1) Wasielewski, M. R. *Chem. Rev.* **1992**, *92*, 435−461.

(2) Barbara, P. F.; Meyer, T. J.; Ratner, M. A. *J. Phys. Chem.* **1996**, *100*, 13148−13168.

(3) De Cola, L.; Belser, P. *Coord. Chem. Rev.* **1998**, *177*, 301−346.

(4) Gust, D.; Moore, T. A. Intramolecular photoinduced electron-transfer reactions of porphyrins. In *The porphyrin handbook*; Kadish, K. M., Smith, K. M., Guilard, R., Eds.; Academic Press: San Diego, 2000; Vol. 8, pp 153−190.

(5) Ort, D. R.; Yocum, C. F. *Oxygenic Photosynthesis. The light reactions*; Ort, D. R., Yocum, C. F., Eds.; Kluwer Academic Publishers: Dordrecht, The Netherlands, 1996.

(6) Hoff, A. J.; Deisenhofer, J. *Phys. Rep.* **1997**, *287*, 1−257.

(7) Kurreck, H.; Huber, M. *Angew. Chem., Int. Ed. Engl.* **1995**, *34*, 849−866.

(8) Harriman, A.; Sauvage, J.-P. *Chem. Soc. Rev.* **1996**, *25*, 41−48.

(9) Gust, D.; Moore, T. A.; Moore, A. L. *Pure Appl. Chem.* **1998**, *70*, 2189−2200.

(10) Kalyanasundaram, K.; Grätzel, M. *Coord. Chem. Rev.* **1998**, *177*, 347−414.

(11) Bard, A. J.; Fox, M. A. *Acc. Chem. Res.* **1995**, *28*, 141−145.

(12) de Silva, A. P.; Gunaratne, H. Q. N.; Gunnlaugsson, T.; Huxley, A. J. M.; McCoy, C. P.; Rademacher, J. T.; Rice, T. E. *Chem. Rev.* **1997**, *97*, 1515−1566.

(13) Helms, A.; Heiler, D.; McLendon, G. *J. Am. Chem. Soc.* **1992**, *114*, 6227−6238.

(14) Osuka, A.; Kobayashi, F.; Maruyama, K.; Mataga, N.; Asahi, T.; Okada, T.; Yamazaki, I.; Nishimura, Y. *Chem. Phys. Lett.* **1993**, *201*, 223−228.

(15) Hunter, C. A.; Hyde, R. K. *Angew. Chem., Int. Ed. Engl.* **1996**, *35*, 1936−1939.

(16) Tsuchiya, S. *J. Am. Chem. Soc.* **1999**, *121*, 48−53.

(17) Knyukshto, V.; Zenkevich, E.; Sagun, E.; Shulga, A.; Bachilo, S. *Chem. Phys. Lett.* **1999**, *304*, 155−166.

(18) DeGraziano, J. M.; Liddell, P. A.; Leggett, L.; Moore, A. L.; Moore, T. A.; Gust, D. *J. Phys. Chem.* **1994**, *98*, 1758−1761.

(19) DeGraziano, J. M.; Macpherson, A. N.; Liddell, P. A.; Noss, L.; Sumida, J. P.; Seely, G. R.; Lewis, J. E.; Moore, A. L.; Moore, T. A.; Gust, D. *New J. Chem.* **1996**, *20*, 839−851.

(20) Osuka, A.; Noya, G.; Taniguchi, S.; Okada, T.; Nishimura, Y.; Yamazaki, I.; Mataga, N. *Chem. Eur. J.* **2000**, *6*, 33−46.

(21) Harriman, A.; Heitz, V.; Sauvage, J.-P. *J. Phys. Chem.* **1993**, *97*, 5940−5946.

10.1021/ja003820k CCC: $20.00
Published on Web 03/13/2001

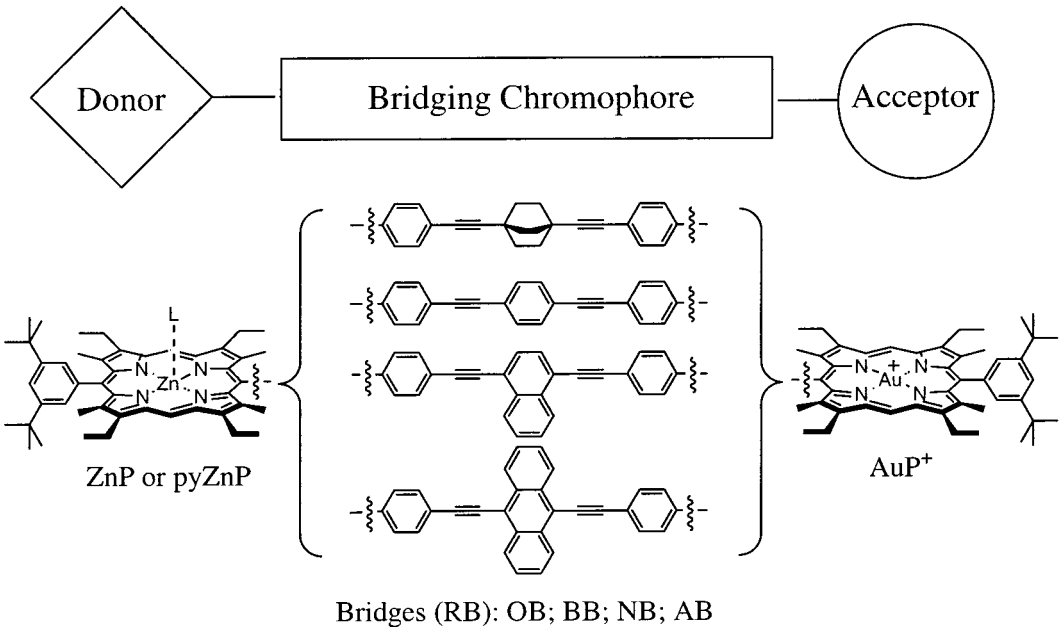

Figure 1. Structure of the systems studied. The donor is either ZnP (no ligand L) or pyZnP (L = pyridine), and the acceptor is AuP^+. The donor−bridge−acceptor (D−B−A) systems are denoted ZnP−RB−AuP^+ or pyZnP−RB−AuP^+, respectively. RB is one of the bridging chromophores: 1,4-bis(phenylethynyl)bicyclo[2.2.2]octane (OB), 1,4-bis(phenylethynyl)benzene (BB), 1,4-bis(phenylethynyl)naphthalene (NB) or 9,10-bis(phenylethynyl)anthracene (AB). The donor reference compounds consist of the porphyrin moiety and the bridging chromophore, D−B.

paramagnetic acceptor.[25] The latter series, with iron(III) porphyrin as acceptor, were synthesized with the expectation that long-range electron transfer would be observed. With the exception of one system in highly polar solvents where stepwise electron transfer via the bridge was observed,[26] it turned out that other deactivation pathways were dominant. We therefore decided to prepare new series designed specifically for electron-transfer studies. These were based on zinc and gold porphyrins as donor and acceptor, respectively, because electron transfer in such systems has previously been observed.

In elegant studies by Harriman, Sauvage, and co-workers, oblique zinc/gold bis-porphyrins of quite short donor−acceptor distance were fully characterized and ET, as well as its temperature dependence, was reported.[21,27,28] In these systems it was shown that electron transfer could occur from both the singlet and triplet excited states of the donor, while hole transfer occurred only from the triplet excited acceptor. Many rotaxane-type compounds with different distances, geometry, and electronic coupling between zinc and gold porphyrins have also been studied.[29−32] Finally, the energy gap dependence of electron transfer has been investigated in noncovalently connected sandwich-like heteroaggregates.[33] In the study presented here, electron transfer from the singlet excited state of the donor has been investigated in a series of porphyrin-based D−B−A systems where only the electronic structure of the bridging chromophores has been varied. Thus, it has been possible to focus on the role of the bridging chromophore on electron transfer and donor−acceptor electronic coupling.

The D−B−A systems we have studied consist of 5,15-diphenyl-2,8,12,18-tetraethyl-3,7,13,17-tetramethyl zinc porphyrin (ZnP) or its pyridine complex (pyZnP) as the donor, and the corresponding gold(III) tetrafluoroborate porphyrin (AuP^+) as the acceptor. The porphyrin moieties are covalently connected by geometrically well-defined bridging chromophores (RB). Three of the four bridging chromophores are fully conjugated systems: a bis(phenylethynyl)arylene where the central arylene is either 1,4-phenylene (BB), 1,4-naphthylene (NB), or 9,10-anthrylene (AB). In the fourth bridging chromophore the conjugation is broken by replacing the arylene with 1,4-bicyclo-[2.2.2]octylene (OB). The general structure of the D−B−A systems is shown in Figure 1. Since these systems are similar in structure to those previously used to investigate the mediating role of the bridge in singlet energy transfer (the donor was ZnP or pyZnP and the acceptor was the corresponding free base porphyrin, H_2P),[22,23] the following characteristics are assumed: (i) The donor−acceptor distance is constant throughout the series (center-to-center 25 Å, edge-to-edge 19 Å). (ii) The relative orientation of the donor and the acceptor is independent of the bridging chromophore. (iii) The spectroscopic identities of the donor, bridge, and acceptor chromophores are preserved in the systems by minimizing the π-conjugation through the D−B−A systems. This is ensured by the placement of methyl groups in the porphyrin β-positions, forcing the porphyrin and adjacent phenyl planes to be almost perpendicular (90° ± 18° at room-temperature according to a Boltzmann distribution on a PM3 calculated surface).

(22) Jensen, K. K.; van Berlekom, S. B.; Kajanus, J.; Mårtensson, J.; Albinsson, B. *J. Phys. Chem. A* **1997**, *101*, 2218−2220.
(23) Kilså, K.; Kajanus, J.; Mårtensson, J.; Albinsson, B. *J. Phys. Chem. B* **1999**, *103*, 7329−7339.
(24) Andréasson, J.; Kajanus, J.; Mårtensson, J.; Albinsson, B. *J. Am. Chem. Soc.* **2000**, *122*, 9844−9845.
(25) Kilså, K.; Kajanus, J.; Larsson, S.; Macpherson, A. N.; Mårtensson, J.; Albinsson, B. *Chem. Eur. J.* In press.
(26) Kilså, K.; Macpherson, A. N.; Gillbro, T.; Mårtensson, J.; Albinsson, B. *Spectrochim. Acta A.* In press.
(27) Harriman, A.; Heitz, V.; Ebersole, M.; van Willigen, H. *J. Phys. Chem.* **1994**, *98*, 4982−4989.
(28) Brun, A. M.; Harriman, A.; Heitz, V.; Sauvage, J.-P. *J. Am. Chem. Soc.* **1991**, *113*, 8657−8663.
(29) Brun, A. M.; Atherton, S. J.; Harriman, A.; Heitz, V.; Sauvage, J.-P. *J. Am. Chem. Soc.* **1992**, *114*, 4632−4639.
(30) Chambron, J.-C.; Harriman, A.; Heitz, V.; Sauvage, J.-P. *J. Am. Chem. Soc.* **1993**, *115*, 7419−7425.
(31) Flamigni, L.; Armaroli, N.; Barigelletti, F.; Chambron, J.-C.; Sauvage, J.-P.; Solladie, N. *New J. Chem.* **1999**, *23*, 1151−1158.
(32) Andersson, M.; Linke, M.; Chambron, J.-C.; Davidsson, J.; Heitz, V.; Sauvage, J.-P.; Hammarström, L. *J. Am. Chem. Soc.* **2000**, *122*, 3526−3527.
(33) Segawa, H.; Takehara, C.; Honda, K.; Shimidzu, T.; Asahi, T.; Mataga, N. *J. Phys. Chem.* **1992**, *96*, 503−506.

Scheme 1

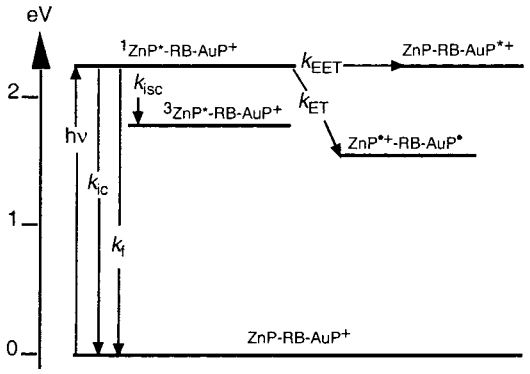

Results

In this study, the main goal has been to investigate the (indirect) influence of the bridging chromophore on electron transfer. We have concentrated on processes that originate from the singlet excited state of the donor zinc porphyrin, and examined the different possible relaxation pathways, such as intersystem crossing $S_1 \rightarrow T_1$, singlet energy transfer to the acceptor, and electron transfer to the acceptor (Scheme 1). The following sections systematically describe the synthesis, the spectroscopic and electrochemical characterization of the compounds, and their photophysical properties.

Synthesis. We have previously synthesized the zinc/free base analogues (ZnP−RB−H_2P) of ZnP−RB−AuP$^+$ by a building block synthesis employing the Sonogashira reaction.[23,34] The compounds linked by aromatic bridge chromophores (R = N, B, A) were prepared from the alkyne-substituted zinc porphyrins **4** and **5** (Scheme 2), and free base iodoporphyrins.[34] The building blocks were connected using the optimized reaction conditions developed by Wagner et al.,[35] i.e. treatment with Pd_2dba_3·$CHCl_3$ (dba is dibenzylideneacetone) and $AsPh_3$ in a mixture of toluene and triethylamine. However, the synthesis of ZnP−OB−H_2P, which went via zinc porphyrin **6**, required the use of the stronger base piperidine because of the lower acidity of alkylacetylenes compared to arylacetylenes.[23]

To prepare the ZnP−RB−AuP$^+$ systems, three different methods were evaluated, all utilizing the gold insertion method recently developed by Chambron et al. for 5,15-diaryloctaalkylporphyrins.[36] In this procedure, $[Au(tht)_2]BF_4$ (tht is tetrahydrothiophene) is used as the metalating agent. The gold insertion takes place by a disproportionation of the Au(I) salt to Au(0) and a Au(III) porphyrin and at least 3 equiv of $[Au(tht)_2]BF_4$ and 2 equiv of base (2,6-lutidine) are required. In the first method, gold insertion into the free base porphyrin moiety of ZnP−RB−H_2P was attempted, analogous to the method used to produce ZnP−RB−FeP from ZnP−RB−H_2P.[25] In the second method, the Sonogashira reaction was used to assemble the ZnP−RB−AuP$^+$ systems from the gold porphyrin (**1**−**3**) and zinc porphyrin (**4**−**6**) building blocks (analogous to the synthesis of ZnP−RB−H_2P).[23,34] Finally, a sequence of gold insertion followed by zinc insertion into a bis(free base porphyrin) dimer was attempted (Scheme 3).

The first method was not successful. When the AB-linked compound, ZnP−AB−H_2P, was subjected to gold insertion with $[Au(tht)_2]BF_4$ (3 equiv) and a 100-fold excess of 2,6-lutidine, to promote the reaction and protect the acid labile zinc porphyrin from demetalation, no gold insertion occurred. Approximately 50% of the starting material could be recovered by chromatography (Al_2O_3/CH_2Cl_2), whereas the remaining part was degraded.[37]

The building block strategy of the second method was feasible, although low-yielding (13−30%). Three of the four ZnP−RB−AuP$^+$ systems (R = O, B, and N) were synthesized with this method. However, since the gold porphyrins have very low solubility in toluene, the reaction conditions developed by Wagner et al.[35] were slightly varied. A yield of 26% was obtained for the phenyl-linked ZnP−BB−AuP$^+$ from **1** and **5** with chloroform as solvent.

In an attempt to increase the yields, we investigated the possibility of using a metal as a cocatalyst. Copper is traditionally used,[38] but we wanted to avoid the risk of transmetalation of the zinc porphyrins,[39] while the gold porphyrins are probably stable toward metal exchange. Copper porphyrins would be troublesome byproducts as they are nonfluorescent, making small amounts of copper porphyrin contaminants hard to detect. Zinc, on the other hand, would be the ideal cocatalyst since exchange of zinc would have no net effect.

Crisp et al. have recently developed a method using $ZnCl_2$ as a cocatalyst together with $Pd(PPh_3)_4$ and NaI in piperidine.[40] This method is especially attractive since piperidine would already be required in the synthesis of ZnP−OB−AuP$^+$ from alkylacetylene **6**.[23] Although we could reproduce their results for the palladium-catalyzed coupling of iodobenzene with phenylacetylene, giving a high yield of diphenylacetylene under mild conditions, this procedure was not as efficient when applied to porphyrins. Coupling of gold porphyrin **2** with zinc porphyrin **4** gave ZnP−NB−AuP$^+$ in a 30% yield (40 °C, overnight). ZnP−OB−AuP$^+$ was afforded in 13% yield from gold porphyrin **1** and zinc porphyrin **6** (80 °C, 6 days). The synthesis of ZnP−AB−AuP$^+$ with the same method failed. The coupling reaction between gold porphyrin **3** and zinc porphyrin **4** (40 °C, 38 h) gave only halide exchange, producing the chloro analogue of **3**, as shown by FAB-MS. Although the coupling reaction can probably be optimized for gold porphyrins, we did not consider it to be within the scope of this investigation. Instead, we sought an alternative way to synthesize ZnP−AB−AuP$^+$.

The third method, starting from a bis(free base porphyrin) dimer (Scheme 3), turned out to be the most convenient. Although a greater number of reaction steps are used, compared to the previous method, the synthetic procedure is easier. This was the method used by Chambron, Sauvage, and co-workers when they applied their gold insertion method to porphyrin stoppered rotaxanes.[41]

ZnP−AB−AuP$^+$ was synthesized from ZnP−AB−H_2P, which was demetalated to H_2P−AB−H_2P. Gold insertion gave a mixture of non-, mono-, and dimetalated dimers, from which H_2P−AB−AuP$^+$ was isolated by chromatography. The separation of the mono- and dimetalated species was surprisingly easy.

(34) Kajanus, J.; van Berlekom, S. B.; Albinsson, B.; Mårtensson, J. *Synthesis* **1999**, 1155−1162.

(35) Wagner, R. W.; Johnson, T. E.; Li, F.; Lindsey, J. S. *J. Org. Chem.* **1995**, *60*, 5266−5273.

(36) Chambron, J.-C.; Heitz, V.; Sauvage, J.-P. *New J. Chem.* **1997**, *21*, 237−240.

(37) A second fraction came off the chromatographic column as a brown smear when MeOH was added to the eluent. This fraction contained a mixture of compounds as judged by TLC. None of the compounds had the chromatographic mobility or appearance of a gold porphyrin.

(38) Sonogashira, K.; Tohda, Y.; Hagihara, N. *Tetrahedron Lett.* **1975**, 4467−4470.

(39) Anderson, H. L.; Sanders, J. K. M. *J. Chem. Soc., Chem. Commun.* **1989**, 1714−1715.

(40) Crisp, G. T.; Turner, P. D.; Stephens, K. A. *J. Organomet. Chem.* **1998**, *570*, 219−224.

(41) Solladié, N.; Chambron, J.-C.; Sauvage, J.-P. *J. Am. Chem. Soc.* **1999**, *121*, 3684−3692.

Scheme 2

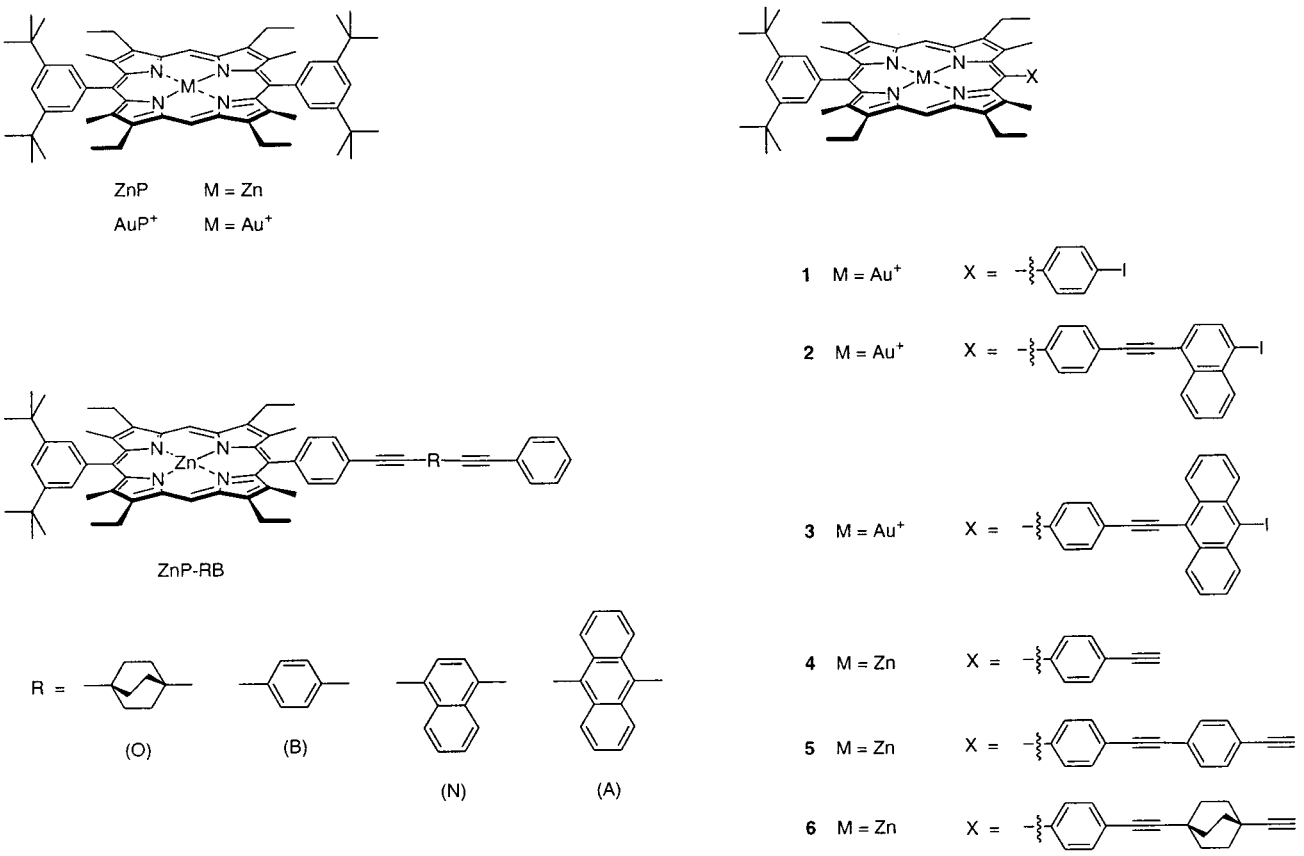

Scheme 3

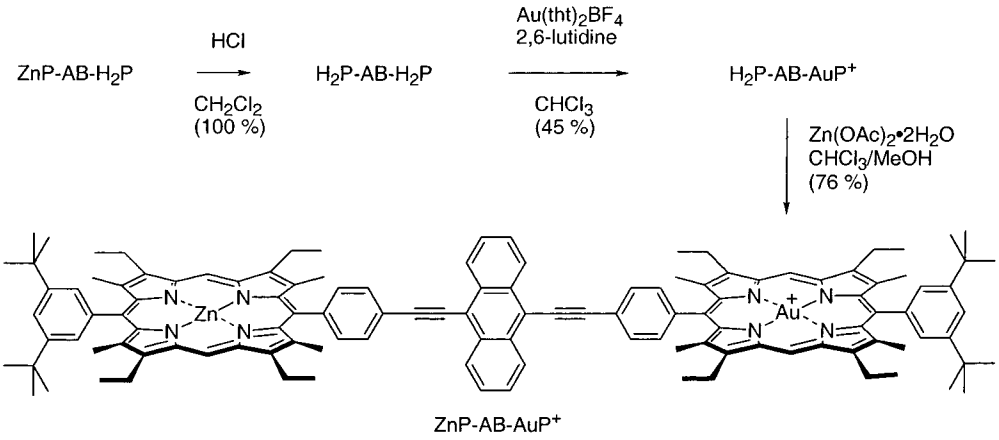

Zinc insertion gave ZnP−AB−AuP$^+$ in 34% overall yield from ZnP−AB−H_2P (Scheme 3). The intermediate H_2P−AB−H_2P could, in principle, be synthesized in a single step by using the palladium-catalyzed reaction between 9,10-diiodoanthracene and an alkyne-substituted free base porphyrin. We did not use this procedure because of the difficulties of removing butadiyne-linked byproducts that may be formed in the palladium-catalyzed reaction.[35] As was pointed out by Lindsey et al.,[42] even if a bis(zinc porphyrin) dimer or a bis(free base porphyrin) dimer is the target molecule, it is advantageous to prepare a mixed zinc/free base porphyrin dimer first. The mixed dimer is easier to purify, and can then be metalated or demetalated. Therefore, we started the synthesis of ZnP−AB−AuP$^+$ from ZnP−AB−H_2P, which was synthesized in a stepwise manner and was free of butadiyne-linked byproducts.[34]

Ground-State Absorption. In the Q-band region of the porphyrins (λ > 500 nm), the absorption spectra of the D−B−A series with zinc porphyrin as a donor are very similar to a linear combination of D−B and A (Figure 2). The absorption maxima in chloroform are seen at 518 and 553 nm for the gold porphyrin acceptor and at 538 and 574 nm (551 and 586 nm upon addition of pyridine) for ZnP and all the bridge-substituted zinc porphyrins. This supports the assumption that D, B, and A can be regarded as isolated chromophores in the D−B−A systems. Although the sum of the components does not match the D−B−A spectra quite as well in the Soret-band region ($\lambda \approx$ 410 nm), the agreement is still satisfactory. The overlap of the donor and acceptor Q-bands and the presence of a AuP$^+$ tail extending into the red means that there is no wavelength where

(42) Lindsey, J. S.; Prathapan, S.; Johnson, T. E.; Wagner, R. W. *Tetrahedron* **1994**, *50*, 8941−8968.

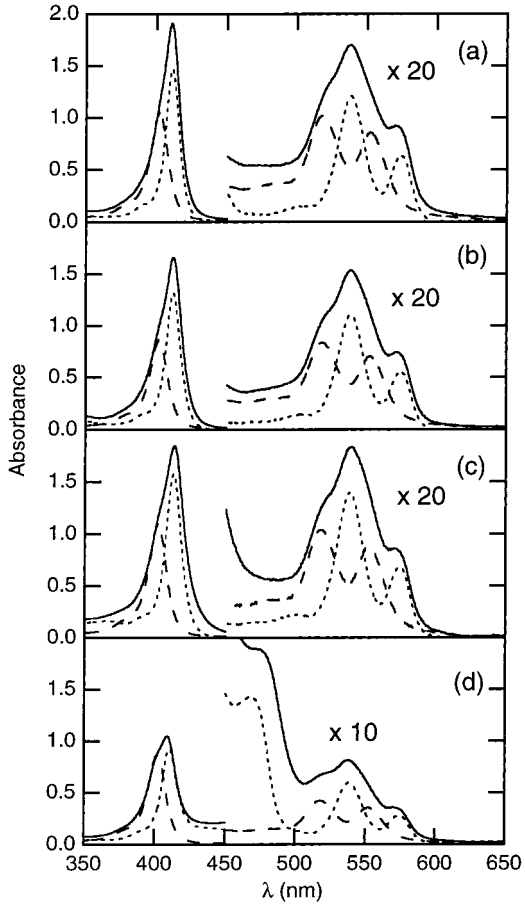

Figure 2. Absorption spectra of the ZnP−RB−AuP$^+$ systems (—), resolved into ZnP−RB (···) and AuP$^+$ (- - -) in $CHCl_3$ at 20 °C. From top to bottom RB is (a) OB, (b) BB, (c) NB, and (d) AB.

ZnP can be selectively excited. In all the fluorescence or transient absorption measurements, the compounds were therefore excited at a wavelength in the Q-band region where the donor absorption dominates. However, since the acceptor has short-lived excited states and is nonfluorescent, excitation of AuP$^+$ will not influence the analysis of the emission properties.

Emission Properties. The steady-state fluorescence spectra of the D−B−A systems show that the donor fluorescence is quenched compared to the D−B reference compounds. The steady-state quenching corresponds to the decrease in the donor lifetime (Table 1). The decrease in both the fluorescence intensity and the lifetime of the singlet excited donor was used to calculate the efficiency (E) and the rate constant (k_{DBA}) for donor quenching.

$$E = 1 - \frac{F}{F_0} = 1 - \frac{\tau_f}{\tau^0_f} \qquad k_{DBA} = \frac{E}{(1-E)\tau^0_f} \qquad (1)$$

F and F_0 are the total donor fluorescence intensities in the D−B−A systems and in the D−B references, respectively, and τ_f and τ^0_f are the corresponding fluorescence lifetimes. The fluorescence lifetimes of the reference compounds were, within experimental error, independent of the bridging chromophore. The efficiencies calculated from the steady-state and time-resolved measurements were, within 20%, the same and the average value was used to calculate k_{DBA}.

In both series, ZnP−RB−AuP$^+$ and pyZnP−RB−AuP$^+$, it is clear that the systems with OB as the bridging chromophore show only a minor quenching, while introduction of aromatic bridging chromophores has a dramatic effect on the donor emission (Figure 3, Table 1). The largest quenching is seen for the AB-bridged systems, followed by the systems with NB and BB as the bridge. In the ZnP−RB−AuP$^+$ series, the donor quenching was measured in solvents of different polarity (although the solubility of the systems in toluene and 2-MeTHF is poor). ZnP−OB−AuP$^+$ showed almost the same rate constant ($k_{DBA} \approx 2 \times 10^8$ s^{-1}) for all solvents. For the other systems, the quenching was dependent upon solvent, with the largest rate constants ($k_{DBA} \approx 2-9 \times 10^9$ s^{-1}) found for the most polar solvents and for the AB-bridged system (Table 2). In the nonpolar solvent toluene, the quenching of the donor emission for the AB-, NB-, and BB-bridged systems was substantially smaller and approached that observed for ZnP−OB−AuP$^+$.

Donor Intersystem Crossing. In a study of a similar D−B−A series with zinc porphyrin as the donor and the paramagnetic high-spin iron(III) chloride porphyrin, FeP, as the acceptor, we found that the presence of this acceptor enhanced the $S_1 \rightarrow T_1$ intersystem crossing rate of the donor contributing significantly to the observed fluorescence quenching.[25] Although AuP$^+$ is diamagnetic and we did not expect the same effect for the systems investigated here, the intersystem crossing could be affected by the heavy-atom effect of gold. This was investigated by using nanosecond transient absorption to detect the amount of triplet formed in D−B relative to D−B−A immediately after the excitation pulse. This was done by comparing the differential absorbances, ΔA_{DBA} and ΔA_{DB}, immediately after the excitation pulse.

In the series with iron porphyrin as the acceptor, a minimum value[43] of enhanced intersystem crossing was determined in the OB-bridged system because triplet energy transfer, which would have complicated the analysis, does not occur in this system.[25] For a similar reason, the OB-bridged system was also chosen to establish if the presence of AuP$^+$ affects the yield of ZnP triplet formation. Assuming that the intersystem crossing quantum yield for ZnP in polar solvents is similar to that reported for zinc tetraphenylporphyrin ($\phi^0_{isc} = 0.90$),[44] the intrinsic rate constant for intersystem crossing is $k^0_{isc} = \phi^0_{isc}/\tau^0_f = 6 \times 10^8$ s^{-1} in butyronitrile. As a result of quenching of the singlet excited donor state in the D−B−A systems, the quantum yield for intersystem crossing, $\phi_{isc} = (\Delta A_{DBA}/\Delta A_{DB})\phi^0_{isc}$, is reduced to 0.78 in ZnP−OB−AuP$^+$. With use of the fluorescence lifetime of ZnP−OB−AuP$^+$, $\tau_f = 1.12$ ns, the rate constant for intersystem crossing, $k_{isc} = 7 \times 10^8$ s^{-1}, is obtained. Since this rate is essentially the same as that for ZnP, within the limits of experimental uncertainty, we do not believe that the donor quenching can be a result of enhanced intersystem crossing in any of the gold porphyrin containing systems.

Energy Transfer. The lowest singlet excited state of AuP$^+$, as determined from the maximum of the lowest energy absorption band (Figure 2), is approximately 700 or 1000 cm^{-1} higher in energy than that in ZnP or pyZnP, respectively. However, since AuP$^+$ is nonfluorescent and the singlet lifetime short, there is no possibility of singlet energy transfer from AuP$^+$ to ZnP or pyZnP. Although energy transfer in the reverse direction, from ZnP or pyZnP to AuP$^+$, does not at first seem likely, the AuP$^+$ absorption has a red tail that overlaps the emission from ZnP and pyZnP (Figure 4). Using Förster theory,

(43) An increase in the rate of intersystem crossing from $(6 \pm 1) \times 10^8$ s^{-1} in ZnP−OB to $(11 \pm 2) \times 10^8$ s^{-1} in ZnP−OB−FeP was determined in 2-methyl-THF. In the systems with the other bridging chromophores the enhancement could be larger, although the results suggested by not more than a factor of 2−3.

(44) Harriman, A.; Porter, G.; Wilowska, A. *J. Chem. Soc., Faraday Trans. 2* **1983**, *79*, 807−816.

Table 1. Fluorescence Intensity (F) and Lifetime (τ) of the Donor Porphyrin Moiety, Together with the Calculated Efficiency (E) and Total Quenching Rate Constant (k_{DBA}) in Chloroform and, in Parentheses, Butyronitrile[a] at 20 °C

compd	F (au)	τ_D (ns)	E[b]	k_{DBA} (s^{-1})	$k_{Förster}$ (s^{-1})
ZnP−OB−AuP$^+$	70 (78)	0.99 (1.12)	0.27 (0.23)	0.3×10^9 (0.2×10^9)	0.1×10^9 (0.1×10^9)
ZnP−OB	100 (100)	1.29 (1.46)			
ZnP−BB−AuP$^+$	18 (20)	0.46 (0.34)	0.73 (0.78)	2.1×10^9 (2.5×10^9)	0.1×10^9 (0.1×10^9)
ZnP−BB	100 (100)	1.28 (1.42)			
ZnP−NB−AuP$^+$	13 (11)	0.37 (0.29)	0.80 (0.85)	3.1×10^9 (3.9×10^9)	0.1×10^9 (0.1×10^9)
ZnP−NB	100 (100)	1.28 (1.47)			
ZnP−AB−AuP$^+$	6	0.21	0.88	5.8×10^9	0.1×10^9
ZnP−AB	100	1.26			
pyZnP−OB−AuP$^+$	83 (86)	0.93 (1.03)	0.20 (0.16)	0.2×10^9 (0.2×10^9)	0.1×10^9 (0.1×10^9)
pyZnP−OB	100 (100)	1.21 (1.25)			
pyZnP−BB−AuP$^+$	5 (20)	0.20 (0.23)	0.89 (0.81)	6.7×10^9 (3.3×10^9)	0.1×10^9 (0.1×10^9)
pyZnP−BB	100 (100)	1.20 (1.30)			
pyZnP−NB−AuP$^+$	5 (14)	0.26 (0.13)	0.87 (0.86)	5.6×10^9 (5.5×10^9)	0.1×10^9 (0.1×10^9)
pyZnP−NB	100 (100)	1.20 (1.12)			
pyZnP−AB−AuP$^+$	3	0.13	0.94	13.2×10^9	0.1×10^9
pyZnP−AB	100	1.19			

[a] Fluorescence measurements were not made in butyronitrile for systems containing AB because of electron transfer from ZnP or pyZnP to AB (see ref 26). [b] Based on an average of steady-state and lifetime measurements.

Table 2. The Refractive Index (n), Dielectric Constant (ϵ), Calculated Driving Force ($\Delta G°$) and Reorganization Energy (λ), Observed Quenching Rate Constants (k_{DBA}), and Calculated Förster Rate Constants ($k_{Förster}$) for ZnP−RB−AuP$^+$ in Different Solvents at 20 °C

solvent	n[a]	ϵ[a]	$\Delta G°$[b] (eV)	λ[c] (eV)	E_{00}[d] (eV)	ZnP−OB−AuP$^+$ k_{DBA}[e] (s^{-1})	ZnP−BB−AuP$^+$ k_{DBA}[e] (s^{-1})	ZnP−NB−AuP$^+$ k_{DBA}[e] (s^{-1})	ZnP-AB−AuP$^+$ k_{DBA}[e] (s^{-1})	ZnP/AuP$^+$ $k_{Förster}$[f] (s^{-1})
toluene	1.496	2.379	0.21	0.26	2.15	$(3.4 \pm 0.7) \times 10^8$	$(0.5 \pm 0.1) \times 10^9$	$(0.8 \pm 0.2) \times 10^9$	$(1.3 \pm 0.3) \times 10^9$	$(2.0 \pm 0.4) \times 10^8$
$CHCl_3$	1.446	4.807	−0.43	0.86	2.15	$(2.9 \pm 0.6) \times 10^8$	$(2.1 \pm 0.4) \times 10^9$	$(3.1 \pm 0.6) \times 10^9$	$(5.8 \pm 1.2) \times 10^9$	$(1.1 \pm 0.2) \times 10^8$
2-MeTHF	1.405	6.97	−0.61	1.08	2.13	$(2.0 \pm 0.4) \times 10^8$	$(1.0 \pm 0.2) \times 10^9$	$(1.6 \pm 0.3) \times 10^9$	$(6.2 \pm 1.3) \times 10^9$	$(1.7 \pm 0.4) \times 10^8$
CH_2Cl_2	1.424	8.93	−0.72	1.13	2.15	$(2.3 \pm 0.5) \times 10^8$	$(2.2 \pm 0.4) \times 10^9$	$(4.3 \pm 0.9) \times 10^9$	$(9.1 \pm 1.8) \times 10^9$	$(1.5 \pm 0.3) \times 10^8$
C_3H_7CN	1.384	24.83	−0.92	1.37	2.13	$(2.2 \pm 0.4) \times 10^8$	$(2.5 \pm 0.5) \times 10^9$	$(3.9 \pm 0.8) \times 10^9$	*g*	$(0.8 \pm 0.2) \times 10^8$
DMF	1.431	38.25	−0.95	1.32	2.12	$(1.3 \pm 0.3) \times 10^8$	$(2.3 \pm 0.5) \times 10^9$	$(4.9 \pm 1.0) \times 10^9$	*g*	$(0.6 \pm 0.1) \times 10^8$

[a] From ref 47. [b] Calculated from eq 5. [c] Calculated from eq 6. [d] Determined from absorption and fluorescence measurements. [e] Uncertainties based on the differences in steady-state and lifetime measurements. [f] Calculated by using eqs 2 and 3. Uncertainties based on uncertainties in lifetime, quantum yield, and molar absorptivity. [g] Not determined due to electron transfer from ZnP to AB in polar and coordinating solvents (see ref 26).

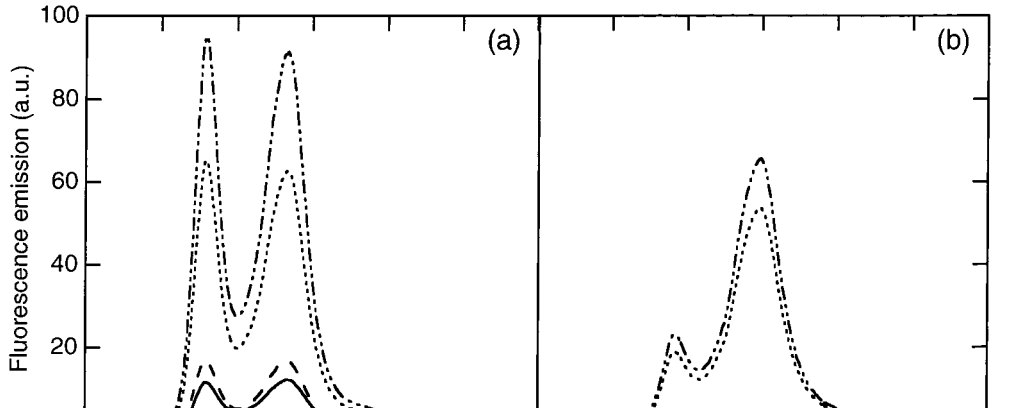

Figure 3. Fluorescence emission spectra of the (a) ZnP−RB−AuP$^+$ ($\lambda_{ex} = 538$ nm) and (b) pyZnP−RB−AuP$^+$ ($\lambda_{ex} = 550$ nm) systems compared to the fluorescence spectrum of the donor alone (scaled to equal donor optical density) in $CHCl_3$ at 20 °C. Donor (- ·· -), RB = OB (···), RB = BB (- - -), RB = NB (—) and RB = AB (- · -).

the expected rate of singlet energy transfer ($k_{Förster}$) in the absence of any mediating influence of the bridge can be calculated.[45,46]

$$k_{Förster} = 8.79 \times 10^{-25} \frac{\phi^0{}_f \kappa^2 J}{\tau^0{}_f n^4 R_{DA}{}^6} s^{-1} \qquad (2)$$

The D−A center-to-center distance (R_{DA}) in our bridged systems is 25.3 Å. The other parameters in this equation are the orientation factor (κ^2), which depends on the orientation of the donor and acceptor transition dipoles, the refractive index of the solvents used (n),[47] and the fluorescence quantum yield ($\phi^0{}_f$) and lifetime ($\tau^0{}_f$) of the donor in the absence of the acceptor. If we assume that the transition dipoles of the metal porphyrin moieties are degenerate in the porphyrin plane[23,48] and the planes

(45) Förster, T. *Naturwissenschaften* **1946**, *33*, 166−175.
(46) Förster, T. *Ann. Phys. (Paris)* **1948**, *2*, 55−75.
(47) *Handbook of Chemistry and Physics*, 75th ed.; CRC Press: Boca Raton, FL, 1994.

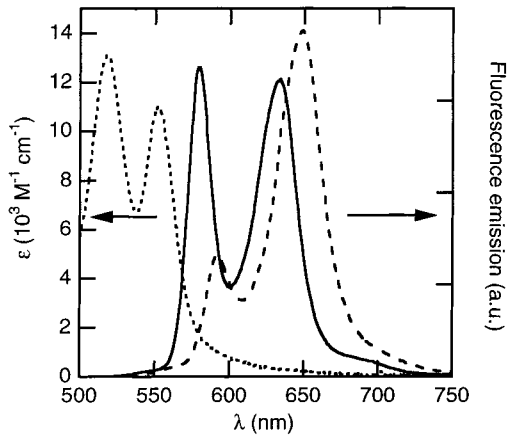

Figure 4. Spectral overlap of AuP^+ Q-band absorbance (···) and normalized ZnP (—) or pyZnP (- - -) emission in $CHCl_3$ at 20 °C.

are almost freely rotating with respect to each other, the average value of $\kappa^2 = 2/3$ for random orientations can be used. The final term is the spectral overlap integral (J), which is calculated from the molar absorptivity of the acceptor ($\epsilon(\lambda)$) and the normalized donor emission ($F(\lambda)$) in the wavelength (λ) region show in Figure 4.

$$J = \int_0^\infty \epsilon(\lambda)\, F(\lambda)\, \lambda^4\, \mathrm{d}\lambda \tag{3}$$

The calculated rate constants for Förster energy transfer are 8×10^7 and $11 \times 10^7\ s^{-1}$ for ZnP−RB−AuP^+ in butyronitrile and chloroform, respectively, and $6 \times 10^7\ s^{-1}$ for pyZnP−RB−AuP^+ in both of these solvents. In the other solvents used to study the fluorescence emission from the ZnP−RB−AuP^+ systems, $k_{\text{Förster}}$ varies between 0.5 and $2 \times 10^8\ s^{-1}$ (Table 2). These calculations indicate that the quenching observed in the OB-linked systems is the result of singlet energy transfer, while in the other systems, an additional pathway must be operating.

Electrochemistry. Cyclic voltammetric measurements were made so that the energy of the charge separated states could be estimated from the redox potentials of the chromophores. The cyclic voltammogram of AuP^+ in CH_2Cl_2 revealed two (reversible) reduction potentials of −1.05 and −1.76 V vs Ag/Ag^+ electrode ($E = 0.45$ vs SHE) at a sweep rate of 100 mV/s. This is in agreement with previously reported data.[36] The oxidation potentials of ZnP and pyZnP are 0.38 and 0.29 V, respectively,[26] indicating a slightly larger driving force for electron transfer in the pyZnP−RB−AuP^+ systems (vide infra). Previously, the AB bridging chromophore has been shown to exhibit reversible potentials: $E_{ox} = 0.86$ V and $E_{red} = -1.68$ V, which is a sufficiently small reduction potential for AB to be a possible electron acceptor (at least on thermodynamic grounds) for the singlet excited states of ZnP and pyZnP.[26] However, for the AB-linked reference compounds, this stepwise ET was only observed in highly polar solvents. BB showed potentials of $E_{ox} = 1.38$ V and $E_{red} = -2.35$ V, while NB gave $E_{ox} = 1.20$ V. The reduction potential for NB was not clearly observed, but if it follows the same trend as for the oxidation potentials, it will lie between BB and AB at approximately −2.1 V.

Electron Transfer. In Marcus theory for diabatic electron transfer, the rate constant for electron transfer (k_{ET}) is related to the electronic coupling (V), the driving force ($\Delta G°$) for the reaction, and the reorganization energy (λ), with contributions from the structure (λ_i) and solvent (λ_s). If V is small compared to λ and the energy of the promoting vibration, the rate constant is given by: [49−51]

$$k_{ET} = \sqrt{\frac{\pi}{\hbar^2 \lambda k_B T}}\,|V|^2 \exp\left(\frac{-(\Delta G° + \lambda)^2}{4\lambda k_B T}\right) \tag{4}$$

where T is the temperature and k_B is the Boltzmann constant. As a result of the quadratic form of $(\Delta G° + \lambda)$, this expression leads to a normal region where k_{ET} increases with more negative $\Delta G°$ and, after a maximum in k_{ET} is reached at $\Delta G° = -\lambda$, an inverted region where k_{ET} decreases with more negative $\Delta G°$.

The calculation of $\Delta G°$ and λ is based on the following parameters: the donor and acceptor redox potentials (E_{ox} and E_{red}), the 0−0 excitation energy of the donor (E_{00}), the donor−acceptor center-to-center distance (R_{DA}), and the average radii of the donor and acceptor (r). The dielectric constant (ϵ_s) and refractive index of the solvent (n) used in the ET measurements, together with the dielectric constant of the solvent used in the electrochemical measurements (ϵ_s^{ref}), are also required:[52−56]

$$\Delta G° = e(E_{ox} - E_{red}) - E_{00} + \frac{e^2}{4\pi\epsilon_0}\left(\frac{1}{\epsilon_s} - \frac{1}{\epsilon_s^{ref}}\right)\left(\frac{1}{r}\right) \tag{5}$$

$$\lambda = \lambda_i + \lambda_s = \lambda_i + \frac{e^2}{4\pi\epsilon_0}\left(\frac{1}{r} - \frac{1}{R_{DA}}\right)\left(\frac{1}{n^2} - \frac{1}{\epsilon_s}\right) \tag{6}$$

In our calculations we have used an average radius of 4.8 Å, as found for other porphyrin-based donor−acceptor systems,[19] and an internal reorganization energy (λ_i) of 0.2 eV, which was used in other systems having zinc and gold porphyrins.[21] Since ET in our systems is a charge transfer, as opposed to a charge separation, we have omitted the Coulombic stabilization term usually present in eq 5. However, inclusion of this term would in the polar solvents only change $\Delta G°$ by 0.1 eV, or less, because the donor−acceptor distance is relatively large. The calculated $\Delta G°$ and λ values for all the solvents studied are listed in Table 2.

Transient Absorption. Transient absorption measurements on the picosecond time scale were made to determine if electron transfer occurs in the systems with π-conjugated bridging chromophores. DMF was chosen for these experiments because its high polarity favors electron transfer and the solubility and stability of the D−B−A systems is high in this solvent. The kinetics recorded at 645 nm and the spectra recorded at 800 ps for the D−B−A systems in DMF are shown in Figure 5a,b. The formation of a clear peak at ∼680 nm, indicative of $ZnP^{\bullet+}$,[13,28] on the time scale of several hundreds of picoseconds for ZnP−BB−AuP^+ and ZnP−NB−AuP^+ is consistent with a dominant electron-transfer quenching pathway for these systems in polar solvents. In contrast, no obvious signal from the radical cation could be detected for ZnP−OB−AuP^+ at 800 ps (Figure

(48) Gouterman, M. Optical spectra and electronic structure of porphyrins and related rings. In *The porphyrins*; Dolphin, D., Ed.; Academic Press: New York, 1978; Vol. III, Chapter 1.

(49) Marcus, R. A. *J. Chem. Phys.* **1956**, *24*, 966−978.

(50) Levich, V. G. Present state of the theory of oxidation−reduction in solution (bulk and electrode reactions). In *Advances in Electrochemisty and Electrochemical Engineering*; Delahay, P., Ed.; Interscience Publishers: New York, 1966; Vol. 4, pp 249−371.

(51) Marcus, R. A.; Sutin, N. *Biochim. Biophys. Acta* **1985**, *811*, 265−322.

(52) Marcus, R. A. *Can. J. Chem.* **1959**, *37*, 155−163.

(53) Marcus, R. A. *J. Chem. Phys.* **1965**, *43*, 679−701.

(54) Rehm, D.; Weller, A. *Ber. Bunsen-Ges. Phys. Chem.* **1969**, *73*, 834−839.

(55) Weller, A. *Z. Phys. Chem. NF* **1982**, *133*, 93−98.

(56) Schmidt, J. A.; Liu, J. Y.; Bolton, J. R.; Archer, M. D.; Gadzekpo, V. P. Y. *J. Chem. Soc., Faraday Trans. 1* **1989**, *85*, 1027−1041.

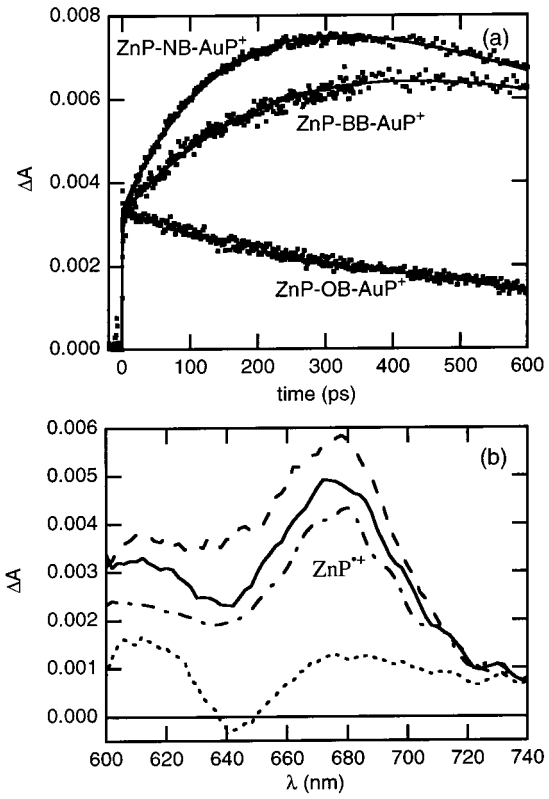

Figure 5. (a) Transient absorption kinetics of ZnP−OB−AuP$^+$, ZnP−BB−AuP$^+$, and ZnP−NB−AuP$^+$ in DMF (λ_{pump} = 585 nm, λ_{probe} = 645 nm). (b) Transient absorption spectra of ZnP−OB−AuP$^+$ (···), ZnP−BB−AuP$^+$ (—), ZnP−NB−AuP$^+$ (- - -), and ZnP−AB−AuP$^+$ (- · -) at 800 ps in DMF (λ_{pump} = 585 nm).

5b). For ZnP−AB−AuP$^+$ in DMF, the major route of ZnP$^{\bullet+}$ formation is by ET to the bridge, giving the charge-separated state ZnP$^{\bullet+}$−AB$^{\bullet-}$−AuP$^+$, followed by a second ET step resulting in ZnP$^{\bullet+}$−AB−AuP$^{\bullet}$. However, in less polar solvents such as CH_2Cl_2 where stepwise ET does not occur,[26] formation of ZnP$^{\bullet+}$ was observed, indicating direct ET in ZnP−AB−AuP$^+$ as is the case for the systems containing BB and NB as bridging chromophores.

Discussion

The donor−bridge−acceptor systems that we have studied were designed to isolate the effect of the bridging chromophore from the other parameters that could influence the rate of electron transfer. To this end, the structure of the donors and acceptor and the overall geometry of the D−B−A systems were kept essentially constant. Previous studies on related systems indicate that both the donor−acceptor distance and relative orientation are independent of the bridging chromophore throughout the series.[22,23] Furthermore, by placement of methyl groups on the porphyrin rings adjacent to the phenyl substituents, direct conjugation through the D−B−A systems is minimized. Although different porphyrin substitution patterns can affect the overall donor/acceptor coupling, as has been found for energy transfer studies of other porphyrin-based systems,[57,58] this does not prevent comparisons of the role of the bridging chromophores being made within our series. Therefore, any change in the quenching rate constant within a series can be directly attributed to differences in the electronic structure of the bridging chromophore, and thus in the electronic coupling between the donor and acceptor.

Two series were investigated, with either the donor ZnP or its pyridine complex pyZnP, and these differed only slightly in their spectroscopic and electrochemical properties. In both series, the lifetime of the singlet excited state of the zinc porphyrin is reduced when the gold porphyrin is covalently linked and the quenching is substantially larger for the fully conjugated bridging chromophores (BB, NB, and AB) compared to the OB-linked systems. Singlet−singlet energy transfer is one of the quenching pathways, although the spectral overlap between the AuP$^+$ absorption and ZnP or pyZnP emission is small. Förster theory was used to calculate a rate constant $k_{Förster} \approx 1 \times 10^8$ s^{-1} for singlet energy transfer in butyronitrile and chloroform, independent of the bridging chromophore. The red shift in the emission spectrum of pyZnP compared to ZnP results in only a small reduction in the Förster energy transfer rate. Experimentally, the reduction in the measured rate constant when changing the donor was only observed for the system with OB as bridging chromophore (Table 1).

In the D−B−A systems previously investigated (D = ZnP or pyZnP, A = free base porphyrin, H_2P), energy transfer rates larger than predicted by the Förster theory ($k_{Förster} = 3.3 \times 10^8$ or 0.9×10^8 s^{-1} for ZnP or pyZnP, respectively) were observed and the enhancement was clearly dependent upon the bridging chromophore.[23] The total rate constant for excitation energy transfer (k_{EET}) could be expressed as $k_{EET} = k_{Förster} + k_{Med}$, where k_{Med} is the mediating contribution from the bridge. For systems with OB, BB, NB, and AB as the bridging chromophore, the average k_{Med} was determined to be 0.5×10^8, 1.7×10^8, 2.2×10^8, and 8.7×10^8 s^{-1}, respectively. Assuming the mediating contribution from the bridge to be the same when AuP$^+$ is the acceptor, the donor quenching rates (k_{DBA}) of Tables 1 and 2 are in reasonable agreement with those expected for singlet energy transfer (k_{EET}) when OB is the bridging chromophore. The contribution from any other quenching pathways, such as electron transfer or enhanced intersystem crossing, must be rather small for ZnP−OB−AuP$^+$. The absence of any significant enhancement in the donor intersystem crossing by the diamagnetic gold porphyrin is not surprising, since this effect has previously only been found for metalloporphyrins with unpaired electrons, such as iron(III) porphyrin[25,59] or copper(II) porphyrin.[60,61]

In contrast to the OB-linked systems, the quenching rate for systems with π-conjugated bridging chromophores is about an order of magnitude larger than the predicted k_{EET} in polar solvents. In the case of toluene, however, the quenching rate is substantially smaller and is of the same order of magnitude as for ZnP−OB−AuP$^+$. The rates in this solvent follow the trend ZnP−AB−AuP$^+$ > ZnP−NB−AuP$^+$ > ZnP−BB−AuP$^+$ > ZnP−OB−AuP$^+$ and correspond, within the experimental uncertainty, to an energy transfer rate constant calculated as the sum of a Förster contribution and bridge mediation. In the more polar solvents, energy transfer must make only a minor contribution to the donor quenching, implying that the electron-transfer pathway is dominant. To directly establish electron transfer as a quenching pathway transient absorption measurements on a picosecond time scale were made in DMF. The zinc porphyrin radical cation, ZnP$^{\bullet+}$, has a characteristic absorption

(57) Strachan, J. P.; Gentemann, S.; Seth, J.; Kalsbeck, W. A.; Lindsey, J. S.; Holten, D.; Bocian, D. F. *J. Am. Chem. Soc.* **1997**, *119*, 11191−11201.

(58) Yang, S. I.; Seth, J.; Balasubramanian, T.; Kim, D.; Lindsey, J. S.; Holten, D.; Bocian, D. F. *J. Am. Chem. Soc.* **1999**, *121*, 4008−4018.

(59) Brookfield, R. L.; Ellul, H.; Harriman, A. *J. Chem. Soc., Faraday Trans. 2* **1985**, *81*, 1837−1848.

(60) Asano-Someda, M.; Kaizu, Y. *Inorg. Chem.* **1999**, *38*, 2303−2311.

(61) Toyama, N.; Asano-Someda, M.; Ichino, T.; Kaizu, Y. *J. Phys. Chem. A* **2000**, *104*, 4857−4865.

band around 680 nm,[13,28] and this spectral feature was only observed for the systems with fully conjugated bridging chromophores. The transient absorption spectrum of ZnP−OB−AuP^+ in the same wavelength region was very similar to that of ZnP at 800 ps. The spectra show a stimulated emission feature at ~645 nm superimposed on a broad and featureless excited-state absorption, typical of the excited singlet state. The direct charge-transfer pathway from ZnP → AuP^+ could not be studied in the ZnP−AB−AuP^+ system in highly polar solvents, because formation of the $ZnP^{\bullet+}$−$AB^{\bullet-}$−AuP^+ charge-separated state is rapid.[26] However, formation of $ZnP^{\bullet+}$ was also observed in CH_2Cl_2, where ET to the bridge does not take place. In view of this and the relatively large quenching rates measured for this system in other solvents, we believe that direct electron transfer to AuP^+ does occur in ZnP−AB−AuP^+, and in all the other systems (including the systems with pyZnP as the donor) with π-conjugated bridging chromophores, in all investigated solvents except toluene.

For ZnP−BB−AuP^+, ZnP−NB−AuP^+, and ZnP−AB−AuP^+ a marked solvent dependence of k_{DBA} is found between toluene and polar solvents. An increase in the rate constant with polarity is indicative of electron transfer in the Marcus normal region. In the nonpolar solvent toluene, the calculated $\Delta G°$ for ET is positive and thus energy transfer is likely to be the only quenching pathway in this solvent, regardless of the bridging chromophore. In butyronitrile and chloroform, where both series (D = ZnP or pyZnP) have been investigated, the rate constant for the systems with fully conjugated bridging chromophores is larger in the systems with pyZnP as the donor. This is consistent with the larger driving force for electron transfer and stabilization of the zinc porphyrin radical cation,[62] and implies that energy transfer, which is expected to decrease upon pyridine coordination, makes a negligible contribution to the total quenching rate constant. The difference between the two series is largest in chloroform, since butyronitrile can also coordinate to ZnP in the same manner as pyridine.

The driving force, $\Delta G°$, depends on the reduction potential of the acceptor, the oxidation potential of the donor, and the energy of the donor's lowest singlet excited state. These are the first terms in eq 5. The oxidation and reduction potentials of the separate donor and acceptor species were measured in dichloromethane and are specific to this one solvent. The driving force for ET in the other solvents in which the photophysics were measured can be estimated by compensating for the change in electrochemical potentials with solvent. A correction for the different solvation energies of the ions can be made by using the solvent dielectric constant and the Born sphere radii of the chromophores involved. This is the last term of eq 5. The validity of using the Born sphere correction has been discussed, in terms of both the spherical shape and the size of the chromophore radii.[56] However, in changing from almost nonpolar to highly polar solvents, we find it appropriate to include this kind of correction. We have used a radius of 4.8 Å, since systems with similar porphyrins showed good agreement between the experimentally determined and calculated driving forces when using this value.[19] In cases where a charge-separated state is formed from a neutral system, a work term is also included in the expression for $\Delta G°$. This term allows for the Coulombic stabilization of the ion pair compared to the separate ions produced in the electrochemical measurements and depends inversely on the distance of D−A charge separation. For our systems, this term is of the order of 0.1 eV and will result in a more negative $\Delta G°$. However, for systems containing gold(III) porphyin, it has been argued that the Coulombic term should not be included because the transfer process is a charge shift ZnP−AuP^+ → $ZnP^{\bullet+}$−$AuP^{\bullet}$.[21,28,30] The reorganization energy of the solvent, λ_s, is also based on the Born sphere radius and distance, and is generally agreed to be of the form found in eq 6.

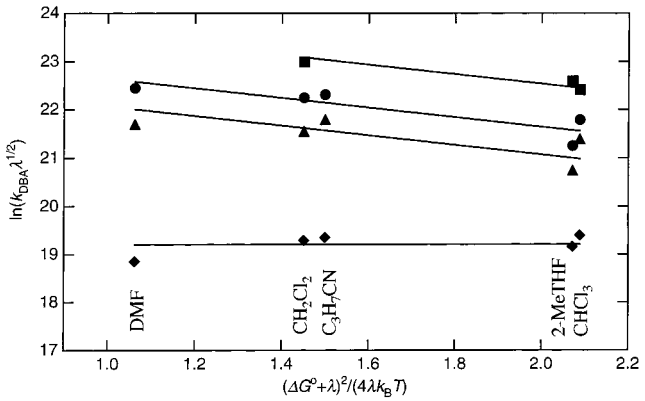

Figure 6. Solvent dependence of k_{DBA} in the ZnP−RB−AuP^+ systems: RB = OB (◆), RB = BB (▲), RB = NB (●), and RB = AB (■). The lines are linear fits with a fixed slope of 0 or −1.

The solvent dependence of k_{DBA} in the polar solvents can be analyzed in several ways, but one simple approach is to rearrange the Marcus equation (eq 4) to a logarithmic form.[56]

$$\ln(k_{ET}\lambda^{1/2}) = \ln\left(\sqrt{\frac{\pi}{\hbar^2 k_B T}}\left|V\right|^2\right) - \frac{(\Delta G° + \lambda)^2}{4\lambda k_B T} \qquad (7)$$

In this way, a plot of $Y = \ln(k_{ET}\lambda^{1/2})$ vs $X = (\Delta G° + \lambda)^2/(4\lambda k_B T)$ should give a straight line with slope −1. Such a plot of the total deactivation rate constant, k_{DBA}, for ZnP−RB−AuP^+ is shown in Figure 6 with the data for toluene omitted. This clearly shows the solvent independence of k_{DBA} in ZnP−OB−AuP^+ (slope 0), compared to the solvent dependence of k_{DBA} in ZnP−BB−AuP^+, ZnP−NB−AuP^+, and ZnP−AB−AuP^+ (slope −1). The lines with fixed slopes fit the data satisfactorily. This therefore supports our assertion that the mechanism for donor quenching in the systems with BB, NB, and AB as bridging chromophores is photoinduced electron transfer from ZnP to AuP^+. The solvent dependence can also yield information about the electronic coupling, V. The couplings calculated from the intercepts of Figure 6 are 6.3, 8.4, and 13.1 cm^{-1} for ZnP−BB−AuP^+, ZnP−NB−AuP^+, and ZnP−AB−AuP^+, respectively. However, there are many parameters that can influence the intercepts determined from this plot, and changing λ_i from 0.2 to 0.1 eV, for example, decreases the coupling by 2−4 cm^{-1}. Including the Coulombic stabilization term in the estimation of $\Delta G°$ also affects the scale of the plot, but not the linearity, and the resulting coupling again decreases 2−4 cm^{-1}.

The data in Figure 6 are based on an average of steady-state and lifetime quenching measurements of fluorescence emission. In general, the steady-state quenching results gave slightly higher rate constants, with the largest difference found for ZnP−AB−AuP^+. This is probably caused by a limitation in the time resolution of our phase/modulation spectrofluorimeter, as the donor quenching efficiency becomes larger than 90%. Calculating the electronic coupling V from the solvent dependence of either the steady-state or lifetime measurements gives the following ranges: ZnP−BB−AuP^+, V = 5.5−7.5 cm^{-1}; ZnP−NB−AuP^+, V = 7−10 cm^{-1}; and ZnP−AB−AuP^+, V = 11−17 cm^{-1}. For an oblique system based on zinc and gold(III)

(62) Gust, D.; Moore, T. A.; Moore, A. L.; Kang, H. K.; DeGraziano, J. M.; Liddell, P. A.; Seely, G. R. *J. Phys. Chem.* **1993**, *97*, 13637−13642.

tetraphenylporphyrins an electronic coupling of 85 cm^{-1} has been found, which decreased to 30 cm^{-1} for the same porphyrin system as part of a rotaxane.[21,30] In this system both the through-space and through-bond (8.5 Å edge-to-edge) distances are much shorter than in the systems presented here. Also the coupling to the bridge in these systems might be larger due to the reduced steric hindrance afforded by the different porphyrin substitution pattern. In view of these differences, the values of the electronic coupling in the ZnP−RB−AuP^+ systems seem reasonable.

The two mechanisms that are generally suggested for ET are the through-space and the through-bond (or superexchange) mechanisms. Because of the large donor−acceptor distance (25 Å center-to-center, 19 Å edge-to-edge) in the systems investigated here, the through-space mechanism, requiring a direct orbital overlap between the donor and acceptor,[63] is not likely to make a contribution. In contrast, the superexchange mechanism, in which virtual states of the bridging chromophore mix with electronic states of the donor and/or the acceptor, can promote long-range electron transfer.[64,65]

The electronic coupling within the superexchange mechanism can be analyzed in terms of the couplings between the donor and bridge, β_{DB}, and between the bridge and acceptor, β_{BA}, and also the energy difference between the initial state and the bridge state involved, δE.[65]

$$V \propto \frac{\beta_{DB}\beta_{BA}}{\delta E} \tag{8}$$

The correlation between V and $1/\delta E$ gives, therefore, a straight line with zero coupling at infinite energy gap. For our systems, δE of the virtual state D^+-B^--A may be calculated as $\delta E = e(E_{ox}^{D} - E_{red}^{B}) - E_{00}^{D}$, an approach that has successfully been used to discriminate between electron and hole transfer in another ZnP/AuP^+ system.[21] However, for our systems a similar calculation of δE fails in two ways. The first is that δE for ZnP−AB−AuP^+ becomes negative for all solvents, even if a solvent correction is included in the same manner as for $\Delta G°$ in eq 5. In highly polar solvents, the negative δE is in agreement with the observed stepwise electron-transfer ZnP → AB,[26] but in the less polar solvents the activation energy for this process is most likely too high and only direct ZnP → AuP^+ electron transfer can occur. The second failure is that a significant (≈4 cm^{-1}), and thus nonzero, coupling for an infinite energy gap is indicated when comparing the ratio of electronic couplings with the ratio of inverse energy gap for BB and NB ($V_{NB}/V_{BB} \approx 1.3$ and $\delta E_{BB}/\delta E_{NB} \approx 1.8$).

We believe that both of these problems have their origin in the fact that δE is calculated from the redox potentials, which are values for the *relaxed* species (including solvent relaxation), and not for the vertical Franck−Condon states, which are involved in the electron tunneling process. Therefore, we will assume that the energy of the virtual bridge state involved in a superexchange mechanism for photoinduced electron transfer is proportional to the LUMO energy of the bridge. For the bridging chromophores investigated here, the first transition is a pure HOMO → LUMO transition and the energy of the LUMO can in our case be shown to be proportional to the energy of the first excited state of the bridge. In our case, we therefore suggest $\delta E \propto E_{00}^{B} - E_{00}^{D}$ to be a better measure of the energy term in the first-order perturbation formulation of the superexchange mechanism (eq 8). The δE values for the systems investigated in this study are 11600, 8600, and 3900 cm^{-1} for ZnP−BB−AuP^+, ZnP−NB−AuP^+, and ZnP−AB−AuP^+, respectively.[23] Figure 7 shows a plot of V vs δE. For the systems with BB and NB as bridges, the correlation including the intercept at zero is very good ($\delta E_{BB}/\delta E_{NB} \approx 1.3$). The deviation of the point for the AB bridge is larger, but so is the experimental uncertainty as a result of the few solvent points in the plot of Figure 6. Furthermore, as has already been mentioned, the measured V could be too small because of the high degree of fluorescence quenching (approaching 100%).

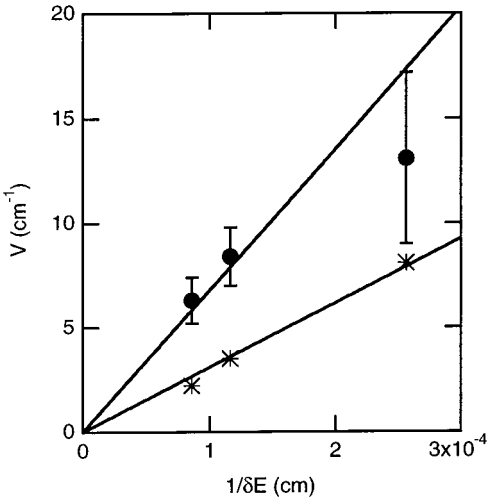

Figure 7. The correlation between the measured (●) or calculated (∗) electronic coupling for electron transfer and the inverse energy gap between the first singlet excited states of the donor and bridge. The lines are the linear fits with a fixed intercept of 0.

The electronic coupling predicted by quantum mechanical calculations on structurally similar, but symmetric, ZnP−RB−ZnP systems[25] is also shown in Figure 7. We believe that ZnP−RB−ZnP is a reasonable model for ZnP−RB−AuP^+ since the absorption spectrum of AuP^+ is similar to that of ZnP (blue-shifted ca. 700 cm^{-1}) and the reduction is believed to be in the porphyrin ring in both cases, rather than at the metal.[66−68]

In the calculations, the electronic coupling for the different bridging chromophores was determined from the minimum energy gap between the near-degenerate LUMO and LUMO# of the entire symmetric D−B−A system. The coupling varies with both the overall conformation of the systems (statistically weighed for a Boltzmann distribution of angles between the porphyrin and phenyl plane) and the relative orientation of the central unit in the bridging chromophore.[23] The (room temperature) couplings obtained on averaging these distributions were 2.2, 3.5, and 8.1 cm^{-1} for RB = BB, NB, and AB, respectively.[25] The electronic couplings estimated from the experimental results are larger than the couplings calculated by a quantum mechanical approach by a factor of 2 to 3, but the relative trend seems to be correctly captured by the theoretical model. The reasonable correlation between the calculated couplings and the measured inverse energy gap δE also indicates that the model based on the bridge excitation energies is reasonable.

The calculations predict that there will be no electronic coupling (0.05 cm^{-1}) in the case of OB as the bridging

(63) Clayton, A. H. A.; Scholes, G. D.; Ghiggino, K. P.; Paddon-Row, M. N. *J. Phys. Chem.* **1996**, *100*, 10912−10918.
(64) McConnell, H. M. *J. Chem. Phys.* **1961**, *35*, 508−515.
(65) Larsson, S. *J. Am. Chem. Soc.* **1981**, *103*, 4034−4040.
(66) Antipas, A.; Dolphin, D.; Gouterman, M.; Johnson, E. C. *J. Am. Chem. Soc.* **1978**, *100*, 7705−7709.
(67) Jamin, M. E.; Iwamoto, R. T. *Inorg. Chim. Acta* **1978**, *27*, 135−143.
(68) Felton, R. H. Primary redox reactions of metalloporphyrins. In *The porphyrins*; Dolphin, D., Ed.; Academic Press: New York, 1978; Vol. V, Chapter 3.

chromophore. For ZnP−OB−AuP^+ the donor−bridge energy gap is 18 000 cm^{-1} which, according to Figure 7, should give a measurable electronic coupling for electron transfer of $V \approx 4$ cm^{-1}. However, for this to be true, it must be assumed that the β values of eq 8 are comparable for the OB and π-conjugated bridges. Since we have shown that ET does not occur in ZnP−OB−AuP^+, this suggests that β is dependent on the type of bridge. It is perhaps not unexpected that the OB systems do not behave in the same manner as the other systems, since the conjugation within the bridge is broken, making the nature of the first excited state of the bridge quite different.[23] OB may be regarded as a series of bridge segments, instead of one bridge, and it will therefore belong to a class of bridging chromophores that is different from the fully conjugated bridges, BB, NB, and AB. It is interesting to note that this observation is in agreement with an investigation of triplet energy transfer in similar systems (ZnP−RB−H_2P, RB = OB, BB, NB). The systems with an OB bridging chromophore showed a rate constant that was remarkably smaller than that of the systems with conjugated bridging chromophores.[24] This qualitative agreement in the mediating effect of the bridge is in accordance with the proposed similarity between triplet energy transfer and electron transfer.[69,70]

Conclusion and Remarks

The D−B−A systems with fully conjugated bridging chromophores that have been described in this work show fast photoinduced electron transfer at a center-to-center distance of 25 Å. When the conjugation within the bridge is broken, the quenching rate constant of the donor is dramatically decreased and the residual quenching corresponds to that expected for singlet−singlet energy transfer. However, energy transfer makes a negligible contribution to the deactivation rate in the systems where electron transfer occurs. In these systems, the electronic coupling of the donor and acceptor is found to be dependent on the bridging chromophore and an inverse relationship with the energy gap between the excited states of the donor and bridge was found. The coupling constants predicted by quantum mechanical calculations showed the same behavior, but were smaller than those determined from the experimental results. These calculations also predict a decrease in coupling with decreasing temperature, and measurements to investigate this are in progress.

Experimental Section

Synthesis. (a) Materials. Triethylamine was dried by distillation from calcium hydride under nitrogen and used immediately after distillation. Commercially available reagents were purchased from Aldrich and used without further purification. The syntheses of the zinc porphyrins **4**−**6** (Scheme 2), ZnP and ZnP−RB, have been described elsewhere.[23,34] AuP^+ was synthesized as described by Chambron et al.[36]

(b) Methods. Column chromatography of the gold porphyrins and ZnP−RB−AuP^+ systems was performed with aluminum oxide (activated, neutral, approximate 150 mesh) deactivated by addition of water to Brockmann grade III.[71] Proton (400 MHz) NMR spectra were recorded at room temperature in $CDCl_3$, using a Varian UNITY-400 NMR spectrometer. Chemical shifts are reported relative to tetramethylsilane (δ_H 0 ppm). Mass spectra were recorded with a VG ZabSpec instrument. The substances were analyzed by positive FAB-MS (matrix 3-nitrobenzyl alcohol) and high-resolution FAB-MS (HRMS) was performed with PEG 1000 as an internal standard. Deaeration of reaction mixtures was achieved by bubbling argon through the solution for 30 min. Palladium-catalyzed coupling reactions were performed under argon and protected from light.

Gold Porphyrin 1. A solution of the free base analogue[34] of **1** (50 mg, 58 μmol), $[Au(tht)_2]BF_4$ (152 mg, 330 μmol), and 2,6-lutidine (27 μL, 232 μmol) in $CHCl_3$ (10 mL) was heated to reflux for 1 h. The solvent was evaporated. The residue was dissolved in CH_2Cl_2 and added to a chromatographic column (Al_2O_3, grade III). Residues of the free base porphyrin were removed by elution with pure CH_2Cl_2. The gold porphyrin was collected by elution with 2% MeOH/CH_2Cl_2. Recrystallization of the gold porphyrin from CH_2Cl_2/hexane gave 44 mg (66%) of **1**. ^{1}H NMR δ 1.52 (s, 18 H, *t*-Bu), 1.83 (t, J = 7.6 Hz, 12 H, $-CH_2CH_3$), 2.57 (s, 6 H, pyrrole-CH_3), 2.65 (s, 6 H, pyrrole-CH_3), 4.13 (q, J = 7.6 Hz, 8 H, $-CH_2CH_3$), 7.82 (dm, J = 8.3 Hz, 2 H, phenyl), 7.85 (d, J = 1.8 Hz, 2 H, phenyl), 7.94 (t, J = 1.8 Hz, 1 H, phenyl), 8.23 (dm, J = 8.3 Hz, 2 H, phenyl), 10.64 (s, 2 H, *meso*); HRMS calcd for $C_{52}H_{59}AuN_4I$ [$(M - BF_4)^+$] 1063.345, found 1063.343.

Gold Porphyrin 2. The free base analogue[34] of **2** was subjected to gold insertion by using the same procedure as described for **1**. Yield 49%. ^{1}H NMR δ 1.53 (s, 18 H, *t*-Bu), 1.85 (m, 12 H, $-CH_2CH_3$), 2.58 (s, 6 H, pyrrole-CH_3), 2.72 (s, 6 H, pyrrole-CH_3), 4.13 (m, 8 H, $-CH_2CH_3$), 7.54−7.69 (m, 3 H, naphthyl), 7.87 (d, J = 1.8 Hz, 2 H, phenyl), 7.95 (t, J = 1.8 Hz, 1 H, phenyl), 8.05 (m, 1 H, naphthyl), 8.10 (d, J = 7.5 Hz, naphthyl), 8.16 (m, 4 H, phenyl), 8.51 (m, 1 H, naphthyl), 10.63 (s, 2 H, *meso*).

ZnP−BB−AuP^+. Pd_2dba_3·$CHCl_3$ (4 mg, 4 μmol) and $AsPh_3$ (10 mg, 32 μmol) were added under argon flushing to a deaerated solution of zinc porphyrin **5**[34] (21 mg, 23 μmol) and gold porphyrin **1** (25 mg, 22 μmol) in 15 mL of $CHCl_3/Et_3N$ (2:1). The reaction mixture was stirred at 40 °C overnight. The solvents were evaporated. The crude product was purified by chromatography on alumina (grade III) eluting with CH_2Cl_2 → 2% MeOH/CH_2Cl_2. The fraction collected with 2% MeOH/CH_2Cl_2 was evaporated and triturated with toluene, removing toluene-soluble material. The residue was recrystallized from CH_2Cl_2/hexane giving 11 mg (26%) of ZnP−BB−AuP^+. ^{1}H NMR δ 1.53 (s, 18 H, *t*-Bu), 1.54 (s, 18 H, *t*-Bu), 1.77 (m, 12 H, $-CH_2CH_3$), 1.84 (m, 12 H, $-CH_2CH_3$), 2.46 (s, 6 H, pyrrole-CH_3), 2.50 (s, 6 H, pyrrole-CH_3), 2.59 (s, 6 H, pyrrole-CH_3), 2.65 (s, 6 H, pyrrole-CH_3), 4.03 (m, 16 H, $-CH_2CH_3$), 7.81 (s, 4 H, phenyl), 7.83 (t, J = 1.8 Hz, 1 H, phenyl), 7.88 (d, J = 1.8 Hz, 2 H, phenyl), 7.94−8.10 (m, 11 H, phenyl), 10.13 (s, 2 H, *meso*), 10.56 (s, 2 H, *meso*); FAB-MS calcd for $C_{114}H_{122}AuN_8Zn$ [$(M - BF_4)^+$] 1863.88, found 1863.88.

ZnP−NB−AuP^+. $Pd(PPh_3)_4$ (3 mg, 3 μmol), $ZnCl_2$ (4 mg, 15 μmol), and NaI (1 mg, 7 μmol) were added under argon flushing to a deaerated solution of zinc porphyrin **4**[34] (9 mg, 11 μmol) and gold porphyrin **2** (7 mg, 5 μmol) in 6 mL of piperidine. The reaction mixture was stirred at 40 °C overnight and then poured into CH_2Cl_2 (20 mL). The organic phase was washed with saturated aqueous NH_4Cl, and the aqueous phase was extracted with CH_2Cl_2 (20 mL). The combined organic layers were dried over Na_2SO_4 and evaporated. The crude product was purified by chromatography on Al_2O_3 (grade III) eluting with CH_2Cl_2 → 2% MeOH/CH_2Cl_2. The fraction collected with 2% MeOH/CH_2Cl_2 was evaporated and triturated with toluene, removing toluene-soluble material. The residue was recrystallized from CH_2Cl_2/hexane giving 3 mg (30%) of ZnP−NB−AuP^+. ^{1}H NMR δ 1.53 (s, 18 H, *t*-Bu), 1.54 (s, 18 H, *t*-Bu), 1.79 (m, 12 H, $-CH_2CH_3$), 1.86 (m, 12 H, $-CH_2CH_3$), 2.46 (s, 6 H, pyrrole-CH_3), 2.58 (s, 6 H, pyrrole-CH_3), 2.60 (s, 6 H, pyrrole-CH_3), 2.72 (s, 6 H, pyrrole-CH_3), 4.02 (m, 8 H, $-CH_2CH_3$), 4.13 (m, 8 H, $-CH_2CH_3$), 7.82−7.87 (m, 3 H, 2 naphthyl + 1 phenyl), 7.89 (d, J = 1.8 Hz, 2 H, phenyl), 7.95 (m, 3 H, phenyl), 8.03 (s, 2 H, naphthyl), 8.11 (d, J = 8 Hz, phenyl), 8.16 (m, 4 H, phenyl), 8.22 (d, J = 8 Hz, phenyl), 8.74 (m, 1 H, naphthyl), 8.78 (m, 1 H, naphthyl), 10.19 (s, 2 H, *meso*), 10.62 (s, 2 H, *meso*); FAB-MS calcd for $C_{118}H_{124}AuN_8Zn$ [$(M - BF_4)^+$] 1913.89, found 1913.90.

ZnP−OB−AuP^+. ZnP−OB−AuP^+ was prepared in 13% yield from **1** and **6** by using the procedure described for ZnP−NB−AuP^+ but employing a higher reaction temperature (80 °C) and a longer reaction time (6 days). ^{1}H NMR δ 1.52 (s, 18 H, *t*-Bu), 1.53 (s, 18 H, *t*-Bu), 1.78 (m, 12 H, $-CH_2CH_3$), 1.83 (m, 12 H, $-CH_2CH_3$), 2.20 (s, 12 H, $-CH_2CH_2-$), 2.45 (s, 6 H, pyrrole-CH_3), 2.50 (s, 6 H, pyrrole-CH_3), 2.58 (s, 6 H, pyrrole-CH_3), 2.64 (s, 6 H, pyrrole-CH_3), 4.01 (m, 8 H, $-CH_2CH_3$), 4.10 (m, 8 H, $-CH_2CH_3$), 7.79−8.02 (m, 14 H, phenyl),

(69) Closs, G. L.; Piotrowiak, P.; MacInnis, J. M.; Fleming, G. R. *J. Am. Chem. Soc.* **1988**, *110*, 2652−2653.
(70) Closs, L. C.; Johnson, M. D.; Miller, J. R.; Piotrowiak, P. *J. Am. Chem. Soc.* **1989**, *111*, 3751−3753.
(71) Brockmann, H.; Schodder, H. *Chem. Ber.* **1941**, *74*, 73−78.

10.17 (s, 2 H, *meso*), 10.58 (s, 2 H, *meso*). FAB-MS calcd for $C_{116}H_{130}AuN_8Zn$ [$(M - BF_4)^+$] 1897.94, found 1897.97.

$H_2P-AB-H_2P$. A solution of the zinc/free base analogue[34] (18 mg) was dissolved in CH_2Cl_2 (70 mL). The solution was extracted with 1 M HCl (50 mL), washed with 5% aqueous $NaHCO_3$ (2 × 50 mL), and dried (Na_2SO_4). Evaporation of the solvent gave the bis(free base porphyrin) dimer in a quantitative yield. ^{1}H NMR δ −2.36 (bs, 4 H, NH), 1.52 (s, 36 H, *t*-Bu), 1.82 (m, 24 H, $-CH_2CH_3$), 2.48 (s, 12 H, pyrrole-CH_3), 2.67 (s, 12 H, pyrrole-CH_3), 4.06 (m, 16 H, $-CH_2CH_3$), 7.82 (t, J = 1.8 Hz, 2 H, phenyl), 7.85 (m, 4 H, anthryl), 7.94 (d, J = 1.8 Hz, 4 H, phenyl), 9.02 (m, 4 H, anthryl), 10.28 (s, 4 H, *meso*). FAB-MS calcd for $C_{122}H_{131}N_8$ [$(M + H)^+$] 1709.05, found 1708.88.

$H_2P-AB-AuP^+$. [Au(tht)$_2$]BF_4 (18 mg, 40 μmol) dissolved in $CHCl_3$ (5 mL) was added to a solution of $H_2P-AB-H_2P$ (17 mg, 10 μmol) and 2,6-lutidine (3 μL, 3 μmol) in $CHCl_3$ (5 mL). The reaction mixture was heated to reflux for 1 h. The solvent was evaporated. The residue was dissolved in CH_2Cl_2 and added to a chromatographic column (Al_2O_3, grade III). Elution with CH_2Cl_2 gave unreacted $H_2P-AB-H_2P$ (5 mg). Elution with 1% MeOH/CH_2Cl_2 gave 9 mg (45%) of $H_2P-AB-AuP^+$. The bis-gold analogue (5 mg) was eluted with 5% MeOH/CH_2Cl_2. ^{1}H NMR δ −2.40 (bs, 2 H, NH), 1.52 (s, 18 H, *t*-Bu), 1.54 (s, 18 H, *t*-Bu), 1.81 (m, 12 H, $-CH_2CH_3$), 1.87 (m, 12 H, $-CH_2CH_3$), 2.49 (s, 6 H, pyrrole-CH_3), 2.60 (s, 6 H, pyrrole-CH_3), 2.66 (s, 6 H, pyrrole-CH_3), 2.79 (s, 6 H, pyrrole-CH_3), 4.05 (m, 8 H, $-CH_2CH_3$), 4.16 (m, 8 H, $-CH_2CH_3$), 7.77 (m, 4 H, anthryl), 7.83 (t, J = 1.8 Hz, 1 H, phenyl), 7.90 (d, J = 1.8 Hz, 2 H, phenyl), 7.94 (d, J = 1.8 Hz, 2 H, phenyl), 7.96 (t, J = 1.8 Hz, 1 H, phenyl), 8.24 (m, 6 H, phenyl), 8.36 (dm, J = 8 Hz, phenyl), 8.88 (m, 4 H, anthryl), 10.26 (s, 2 H, *meso*), 10.65 (s, 2 H, *meso*). FAB-MS calcd for $C_{122}H_{128}AuN_8$ [$(M - BF_4)^+$] 1903.00, found 1903.01.

$ZnP-AB-AuP^+$. $Zn(OAc)_2 \cdot H_2O$ (10 mg, 46 μmol) dissolved in MeOH (1 mL) was added to a solution of $H_2P-AB-AuP^+$ (9 mg, 4.5 μmol) in $CHCl_3$ (5 mL). The reaction mixture was stirred at room temperature for 2.5 h and diluted with $CHCl_3$ (30 mL). The organic layer was washed with 5% aqueous $NaHCO_3$ (2 × 30 mL) and water (30 mL), dried (Na_2SO_4), and evaporated. The crude product was purified by chromatography (Al_2O_3, grade III) eluting with $CH_2Cl_2 \rightarrow$ 4% MeOH/CH_2Cl_2. The fraction collected after addition of MeOH to the eluent was recrystallized from CH_2Cl_2/hexane giving 7 mg (76%) of $ZnP-AB-AuP^+$. ^{1}H NMR δ 1.53 (s, 18 H, *t*-Bu), 1.55 (s, 18 H, *t*-Bu), 1.80 (m, 12 H, $-CH_2CH_3$), 1.87 (m, 12 H, $-CH_2CH_3$), 2.46 (s, 6 H, pyrrole-CH_3), 2.60 (s, 6 H, pyrrole-CH_3), 2.63 (s, 6 H, pyrrole-CH_3), 2.78 (s, 6 H, pyrrole-CH_3), 4.03 (m, 8 H, $-CH_2CH_3$), 4.14 (m, 8 H, $-CH_2CH_3$), 7.80 (m, 4 H, anthryl), 7.83 (t, J = 1.8 Hz, 1 H, phenyl), 7.90 (d, J = 1.8 Hz, 2 H, phenyl), 7.96 (m, 3 H, phenyl), 8.22 (m, 6 H, phenyl), 8.35 (dm, J = 8 Hz, phenyl), 8.92 (m, 4 H, anthryl), 10.20 (s, 2 H, *meso*), 10.64 (s, 2 H, *meso*). FAB-MS calcd for $C_{122}H_{126}AuN_8Zn$ [$(M - BF_4)^+$] 1965.91, found 1965.88.

Spectroscopic Measurements. All solvents (CH_2Cl_2, *N*,*N*-dimethylformamide (DMF) (from LabScan), $CHCl_3$, butyronitrile (from Merck), and 2-methyltetrahydrofuran (2-MeTHF) (from Acros)) were used as purchased. All measurements were made at 20 °C. Pyridine (from LabScan) was distilled before use. Samples containing pyZnP were prepared immediately before spectroscopic measurements by adding pyridine to the corresponding ZnP solution. At a final pyridine concentration of approximately 2 M full conversion of ZnP to pyZnP was obtained, as judged from the changes in the absorption spectra.[26] Pyridine does not coordinate with AuP^+.

Absorption spectra were recorded on a Cary 4 Bio spectrophotometer. Fully corrected steady-state emission spectra were recorded on a SPEX Fluorolog τ2 spectrofluorimeter. Quantum yields were determined relative to ZnP in chloroform (0.025).[23,26] The concentration of the chromophores was kept at approximately 5 μM to exclude the possibility of intermolecular interactions and to ensure that inner filter effects were negligible. To facilitate immediate comparison of the emission spectra of the D−B−A systems, the optical densities of the samples were matched at the excitation wavelength (537−550 nm, dependent upon solvent).[26] The emission spectra of the reference compounds (D−B) were numerically scaled to take into account the partitioning of the incident excitation light between the donor and the acceptor in the D−B−A systems. The quenching efficiency was calculated from the decrease in the integrated intensity of the donor emission.

Fluorescence lifetimes were measured by the phase/modulation technique on a SPEX Fluorolog τ2 spectrofluorimeter, with a diluted silica sol scattering solution as the reference. On a logarithmic scale in the range 10−300 MHz, 20 modulation frequencies were selected and the emission was collected through a 550 nm cutoff filter. The 528.7 nm line from an argon laser (Spectra Physics 165-08) was used as excitation source, except for samples containing AB or pyZnP, where the 514.5 nm line was used. For all the compounds (D−B−A and D−B), the observed demodulations and phase shifts could be satisfactorily fitted to a single-exponential model since the acceptor is nonfluorescent. However, even better fits for the D−B−A systems were found if a small fraction (5−10%) was fitted to a much longer lifetime, irrespective of compound. This is most likely due to impurities or instrumental artifacts. Including this second lifetime did not change the donor lifetime significantly. The goodness-of-fit was evaluated from the value of χ^2 and by visual inspection of the fit to the data points. In frequency domain measurements it is not the absolute value of χ^2, but rather the relative change in χ^2 with different models, that is used as an indication of goodness-of-fit.[72]

Transient absorption kinetic traces on the nanosecond time scale were measured as described previously on an Applied Photophysics flash photolysis instrument.[25] The pump pulse was the second harmonic of a Nd:YAG laser (Spectron Laser Systems, SL803G, 532 nm) with a pulse width of about 10 ns fwhm. The concentration of the samples was approximately 5 μM. However, in the analysis, differences in donor absorbance were corrected for. Butyronitrile was used as the solvent, and all samples were degassed by 5 freeze−pump−thaw cycles to a final pressure of 10^{-4} mbar.

Transient absorption spectra on the picosecond time scale were made by using the pump−probe technique with the setup described previously.[25] Excitation pulses at 585 nm and a 5 kHz repetition rate were provided by frequency doubling the signal output of an optical parametric amplifier (Spectra Physics, OPA-800) pumped by a Ti:Sapphire regenerative amplifier (Positive Light, Spitfire). Transient absorption spectra were recorded between 470 and 740 nm with a 2 nm step size. Kinetics were determined over an 800 ps time range (the maximum available with the setup) and thus charge recombination times could not be reliably determined. The sample was held in a static 1 mm path length cuvette and the concentration was approximately 160 μM in DMF.

Cyclic Voltammetry. The redox potentials of AuP^+, BB, and NB were measured in a similar way as described earlier for AB, ZnP, and pyZnP by using a PAR 273A potentiostat with a platinum working electrode, a platinum coil counter electrode, and a double junction Ag/Ag^+ reference electrode (E = 0.45 V vs SHE).[26] The chromophores were dissolved in CH_2Cl_2 to a concentration of 1 mM (AuP^+) or 2 mM (BB and NB), with 0.1 M $(Bu)_4NBF_4$ as supporting electrolyte. The solutions were N_2-purged before measurement and the sweep rates varied between 0.1 and 1 V/s.

Acknowledgment. This work was supported by grants from the Swedish Natural Science Research Council (NFR) and the Swedish Research Council for Engineering Sciences (TFR). K.K. is grateful to the Danish Research Agency in Århus for a fellowship. We thank Dr. Gunnar Stenhagen for help concerning mass spectrometry and Prof. Elisabeth Ahlberg for help with the electrochemical measurements.

JA003820K

(72) Lakowicz, J. R. *Principles of fluorescence spectroscopy*, 2nd ed.; Kluwer Academic/Plenum Publishers: New York, 1999.